NANO LETTERS

LETTER

pubs.acs.org/NanoLett

Transistor-like Behavior of Single Metalloprotein Junctions

Juan M. Artés,[†,‡] Ismael Díez-Pérez,[‡,†] and Pau Gorostiza*[,†,§,⊥]

[†]Institute for Bioengineering of Catalonia (IBEC), Baldiri Reixac 15-21, Barcelona 08028 Spain

[‡]Physical Chemistry Department, University of Barcelona (UB), Martí i Franquès 1-11, Barcelona 08028 Spain

[§]Networking Research Center on Bioengineering, Biomaterials and Nanomedicine (CIBER-BBN)

[⊥]Institució Catalana de Recerca i Estudis Avançats (ICREA)

Supporting Information

ABSTRACT: Single protein junctions consisting of azurin bridged between a gold substrate and the probe of an electrochemical tunneling microscope (ECSTM) have been obtained by two independent methods that allowed statistical analysis over a large number of measured junctions. Conductance measurements yield $(7.3 \pm 1.5) \times 10^{-6} G_0$ in agreement with reported estimates using other techniques. Redox gating of the protein with an on/off ratio of 20 was demonstrated and constitutes a proof-of-principle of a single redox protein field-effect transistor.

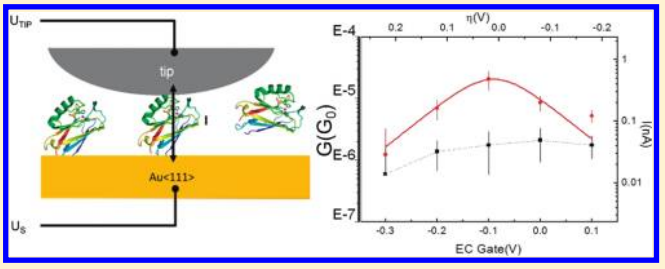

KEYWORDS: Redox protein, STM, molecular electronics, molecular junctions, electrochemical gate, azurin transistor

The study of biological electron transfer (ET) is fundamental to understand important cellular processes like respiration and photosynthesis,[1] and in recent years it has exhibited a rapidly growing relevance in technological applications. The design of efficient ET pathways between the electrocatalytic center of redox enzymes and the electrode allows the use of redox mediators and other reagents to be overcome[2,3] and has led bioelectrochemical redox enzyme sensors to achieve widespread clinical applications in humans including subcutaneous implants for continuous glucose monitoring[2] and to dominate the drug development and clinical sensor industry.[4]

Redox proteins are also emerging as building blocks of molecular bioelectronic devices like logic gates[5] and robust multistate memory devices based on redox protein heterolayers.[6] Strategies to couple redox enzymes to solid electrodes and nanoparticles are well characterized,[7] and the electrochemical properties of these proteins can be exquisitely tuned.[8,9] At the ultimate level of miniaturization, each device would be constituted by a single protein. However, little is known about their electronic and electrochemical properties and about their statistical behavior at this scale, which is essential for device implementation and performance.

Several techniques have been devised to study changes in fluorescence following ET in individual redox enzymes.[10−13] ET can also be investigated by electrochemical scanning tunneling microscopy (ECSTM) which shows that the apparent height of individually resolved redox proteins changes with the overpotential of the ECSTM electrodes, as a result of a redox gate effect on the protein tunneling conductance.[14−16] Here we report a method to directly measure ET currents with individual redox proteins bridged between two electrodes that allows the statistical analysis of their ET properties over hundreds of molecules in each experiment. Our approach is based on the application of molecular break junctions[17] (BJ), a technique to measure single molecule conductance[18,19] that pioneered the field of molecular electronics.[20]

These tools have been used to characterize hydrocarbon chains,[18,19] compounds bearing redox groups,[21,22] and DNA.[23−26] However, their application to more complex redox biomolecules has not been reported besides studies of solid state protein junctions in air[27,28] and reports on small peptide junctions.[29,30]

Single-protein conductance was measured with an ECSTM using the STM-BJ approach[18] on the blue copper protein azurin (Az) in buffer solution and under bipotentiostatic control. Azurin is a widely studied redox protein model[31] that has a globular structure containing a copper ion coordinated by protein residues.[32] This redox center makes the protein capable of accepting and transporting electrons by switching its redox state ($Cu^{I/II}$) and supports its role as a soluble electron carrier in the respiratory chain of bacteria. Briefly, experiments were carried out on azurin bound to an Au ⟨111⟩ substrate via native cysteine residues as described.[14−16,15] The ECSTM probe was approached toward and retracted from the substrate while recording the probe current (see diagram in Figure 1a). In a coherent electron tunneling process, the rate of ET is proportional to an exponential function of the distance between an electron donor and an acceptor[1] (d_{AB} in eq 1) with a distance decay factor β that is characteristic of the medium separating both donor and acceptor sites. In the case of single-molecule junctions, the β

Received: August 21, 2011
Revised: October 3, 2011
Published: October 05, 2011

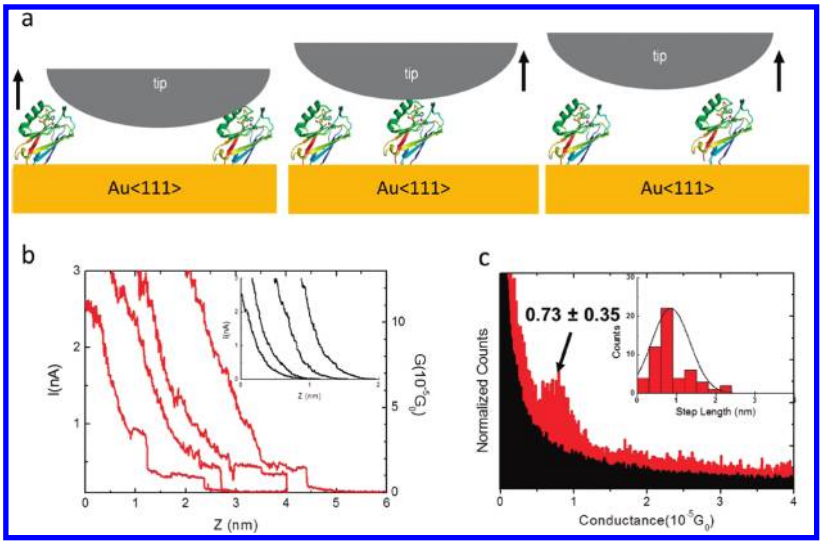

Figure 1. (a) Schemes of a single-azurin junction formation by the STM-BJ approach. The ECSTM probe is approached to the surface and retracted afterward. Eventually a single azurin bridges the two electrodes. (b) Raw data examples of $I(z)$ plots exhibiting current plateaus or steps corresponding to single azurin junction formation. The conductance values are represented in the right axis ($G_0 = 2e^2/h \approx 77.4\,\mu$S). The inset shows curves obtained on a clean gold surface. A horizontal offset was applied in all of them for clarity. (c) Conductance histogram for azurin (in red) obtained from 500 $I(z)$ plots by the STM-BJ approach. The histogram obtained in a clean gold surface is superimposed in black. The inset shows the step length histogram obtained from 50 $I(z)$ plots displaying a maximum centered at 0.85 ± 0.55 nm. The experiments were performed in 50 mM ammonium acetate solution (pH 4.5) at $U_P = -0.1$ V vs SSC, $U_S = 0.2$ V vs SSC, and $U_{bias} = U_P - U_S = -0.3$ V.

decay will be dominated by the molecular structure.

$$k_{ET} \propto \exp(-\beta d_{AB}) \quad (1)$$

We reported that current−distance $I(z)$ measurements at fixed probe (U_P) and substrate potentials (U_S) decay exponentially in the tunneling range, in agreement with eq 1, and yield β = 10 nm^{-1} for clean gold and β = 3−4 nm^{-1} for azurin, which is consistent with a two-step long-range ET mechanism.[33] Similar distance decay factors have been reported by other groups[34] and confirmed theoretical predictions[35] for a multistep tunneling process. When $I(z)$ plots are acquired repetitively, about 10% of the recordings display current plateaus and discrete steps that resemble those reported for small organic compounds using the same setup.[18,19,21] Current steps (shown in Figure 1b) are absent in $I(z)$ plots obtained in control experiments on clean gold (inset of Figure 1b) and thus were interpreted as transient formation and rupture of molecular junctions with azurin bridging the two electrodes (the Au substrate and ECSTM probe). Such "wired" molecular junctions are distinct from tunneling junctions reported in electrochemical tunneling microscopy and spectroscopy measurements.[14,33,34,36] The conductance of these events can be calculated from the current step level as $G = I_{step}/U_{bias}$ in a moderate bias range.[18] Statistic analysis of 500 $I(z)$ curves containing steps allows building a conductance histogram (Figure 1c) in which peaks correspond to current plateaus in the $I(z)$ plots.[37] The conductance histogram for azurin (red plot in Figure 1c) displays a peak that can be fit with a Gaussian distribution function and yields an average conductance of (7.3 ± 3.5) × 10$^{-6}G_0$ (where $G_0 = 2e^2/h \approx 77.4\,\mu$S). The histogram for a clean gold sample decays monotonically and is plotted in black in Figure 1c as a control. This result is in general agreement with conductance estimates using conductive atomic force microscopy in air[38,39] and protein immobilization at the ECSTM probe apex under potentiostatic control.[36] Recent estimates of cytochrome conductance lie within the same range.[16] Since the protein orientation in the junction is fixed by the substrate-bonded native cysteines C3 and C26,[34] we speculate that covalent bonds are also established with the ECSTM probe during approach−retract cycles, probably mediated by charged residues on the protein surface (e.g., amines). The most likely candidate for this interaction is the region surrounding residue K41. This lysine is exposed to the solvent at a region facing the probe and opposite to substrate-bonded C3 and C26, and it aligns well with the sequences of gold- and platinum-binding peptides reported in the literature[40] (see Figure S1, Supporting Information). As explained in Experimental Methods (Supporting Information), Au probes were used in most experiments and no significant differences were observed with Pt−Ir probes. Although the nature of the tip−azurin interaction needs to be fully clarified, the relatively long step length of the observed current plateaus in the $I(z)$ plots of Figure 1b (∼1 nm, see inset in Figure 1c) is comparable to previous measurements with large synthetic molecular systems of similar molecular length covalently bridged between two electrodes.[41] This fact suggests a seemingly stable interaction between our STM probe and the azurin that provides a good electronic coupling and a fairly high conductance value for the single-protein junction. To look further into the STM probe−azurin electronic coupling, $I(U_{bias})$ characteristics of the single-protein junction were recorded using the $I(t)$ method described below. The slope of $I(U_{bias})$ plots in the linear region at low bias potentials (see Figure S2, Supporting Information) yields a conductance value of (1 ± 0.2) × 10$^{-5}G_0$, in very good agreement with the conductance obtained from $I(z)$ histograms (Figures 1 and 2). This fact is evidence of the formation of a stable single-molecule junction that remains all along the bias potential excursion. Moreover, the asymmetry between the positive and the negative branches of the $I(U_{bias})$ plot at high bias provides a measure of the difference in electronic coupling between one side of the molecular bridge (where a strong thiol covalently bonds azurin to the gold substrate) and the

dx.doi.org/10.1021/nl2028969 |Nano Lett. 2012, 12, 2679–2684

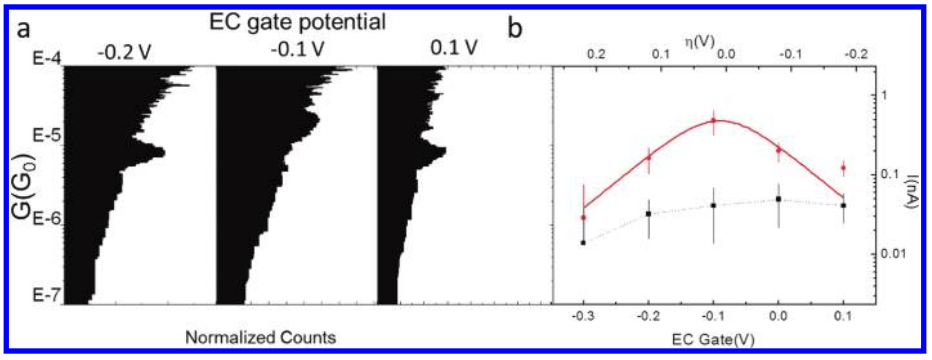

Figure 2. (a) Semilogarithmic conductance histograms obtained from azurin experiments at different electrochemical gate voltages ($-U_S$ in our ECSTM system) and constant bias conditions ($U_{bias} = U_P - U_S = -0.3$ V). (b) Conductance values obtained from the center of the Gaussian fit of the histograms peaks as a function of EC gate potential at constant −0.3 V bias for azurin (red circles) and nonredox Zn−azurin junctions (black squares). Upper axis represents overpotential ($\eta = U_S - U_{AZ}$). Error bars indicate the full width half-maximum (fwhm) of the Gaussian fit on each conductance peak. The red plot shows a fit of the numerical version[45] corresponding to the formalism for a two-step electron transfer process.[14] Control measurements with non-redox Zn−Az are indicated with a dashed black line as visual guidance (see Figure S4 in the Supporting Information). All experiments were performed in 50 mM ammonium acetate solution (pH 4.55).

opposite side (where azurin forms a weaker bond with the Au or Pt STM probe).[42] The current at ±1 V bias in Figure S2 (Supporting Information) is only a factor of 2 higher in the positive branch than in the negative branch of the $I(U_{bias})$ plot, which corroborates the good electronic coupling achieved between the STM probe and azurin. Similar low asymmetries in $I(U)$ characteristics from molecular junctions have been ascribed to different contact geometries on individual runs[43] and to an asymmetric position of an acceptor group within the molecular backbone,[44] the latter being a similar scenario to our single-azurin junction where the Cu(I) center is asymmetrically located versus both electrodes at the junction.[32]

To our knowledge, this is the first report of single protein junction conductance measurements by the ECSTM-BJ approach. We then asked whether the single-azurin junction conductance is modified with the redox state of the protein. The Cu redox center of azurin plays a key role in the ET process[14,15,33,34] that has been studied at the single molecule level by analyzing the effect of electrode potentials on ECSTM imaging,[14,15,33] by current−voltage,[36] and by current−distance spectroscopies.[33] The single azurin junction conductance is thus expected to depend on the electrochemical potentials of the probe and substrate electrodes. To test this hypothesis, we recorded $I(z)$ curves at different probe (U_P) and substrate (U_S) potentials, using a −0.3 V constant bias potential ($U_{bias} = U_P - U_S$). This experiment is equivalent to previous use of the electrochemical potential as the gate voltage to modulate the current in single-molecule junctions employing a ECSTM configuration.[45−47] Here, the voltage of the reference electrode is tuned to modulate the gate voltage in analogy to the gate electrode in a field effect transistor (FET). As the STM probe is grounded in our STM electronic configuration, the EC gate will be equal to $-U_S$ at given U_{bias}. Figure 2a shows semilogarithmic conductance histograms at different EC gate potentials (see Figure S3 in the Supporting Information for linear conductance histograms). Notice the shift in the conductance peak toward higher conductance values as the EC gate potential approaches −0.1 V. This potential corresponds to $U_S = 0.1$ V vs SSC, a value close to the azurin standard potential ($U_{Az} = 0.08$ V vs SSC). Average conductance values obtained as function of the EC gate potential are plotted in Figure 2b (red circles). The maximum conductance value ($(2.1 \pm 0.7) \times 10^{-5} G_0$) occurs at −0.1 V EC gate potential, close to zero overpotential (see upper axis in Figure 2b, where $\eta = U_s - U_{Az}$) that corresponds to the alignment of the Fermi levels of the electrodes with the azurin redox level. In contrast, the conductance of a non-redox Zn−Az control obtained at the same potentials is similar ($10^{-6} G_0$) but does not depend on electrochemical potential (black squares in Figure 2b). This supports the idea that the redox center assists the ET process in the known multistep tunneling process,[14,15,33] even in this molecular junction configuration. The observed dependence on potentials demonstrates that the conductance in the junction is characteristic for redox Cu−azurin, as non-redox Zn−azurin control shows no electrochemical gate dependence. The conductance values obtained for Zn−Az are in the same range as the ones obtained at high electrochemical gate, i.e., high-overpotential conditions, for Cu−Az, which correspond to conductance through the protein backbone, i.e., not assisted by the metal center.[48]

Notice the 20-fold on/off ratio in the conductance between zero and high-electrochemical gate voltages. This value is slightly higher than that reported for azurin in ECSTM configuration[14,36] and about half of the ratio reported for transition metal complexes.[22]

Results of azurin conductance can be expressed in terms of current intensity measured in the junction as function of applied overpotential (red circles in Figure 2b referred to right and upper axes). In order to have more information about the ET mechanism in these molecular junctions, the results were fitted using the numerical approximation[46] for a two-step ET model[14] (eq 2, red line in figure 2b).

$$I = \frac{910 U_{bias} \exp[-9.73(\lambda + U_{bias})]}{\cosh[19.4(\xi\eta + (\gamma - 1/2)U_{bias})]} \quad (2)$$

where I is the current intensity expressed in nanoamperes, U_{bias} is the tip bias voltage, and η is the overpotential given in volts, λ is the reorganization energy in electronvolts, and ξ and γ are two parameters describing the shift of the effective electrode potential at the redox center with the variation of η and U_{bias}, respectively.[46] Fitting the experimental data (red circles in Figure 2b) to this model yields $\lambda = 0.35$ eV, $\xi = 0.79$, and $\gamma = 0.53$. These results are in agreement with values reported for

dx.doi.org/10.1021/nl2028969 |Nano Lett. 2012, 12, 2679–2684

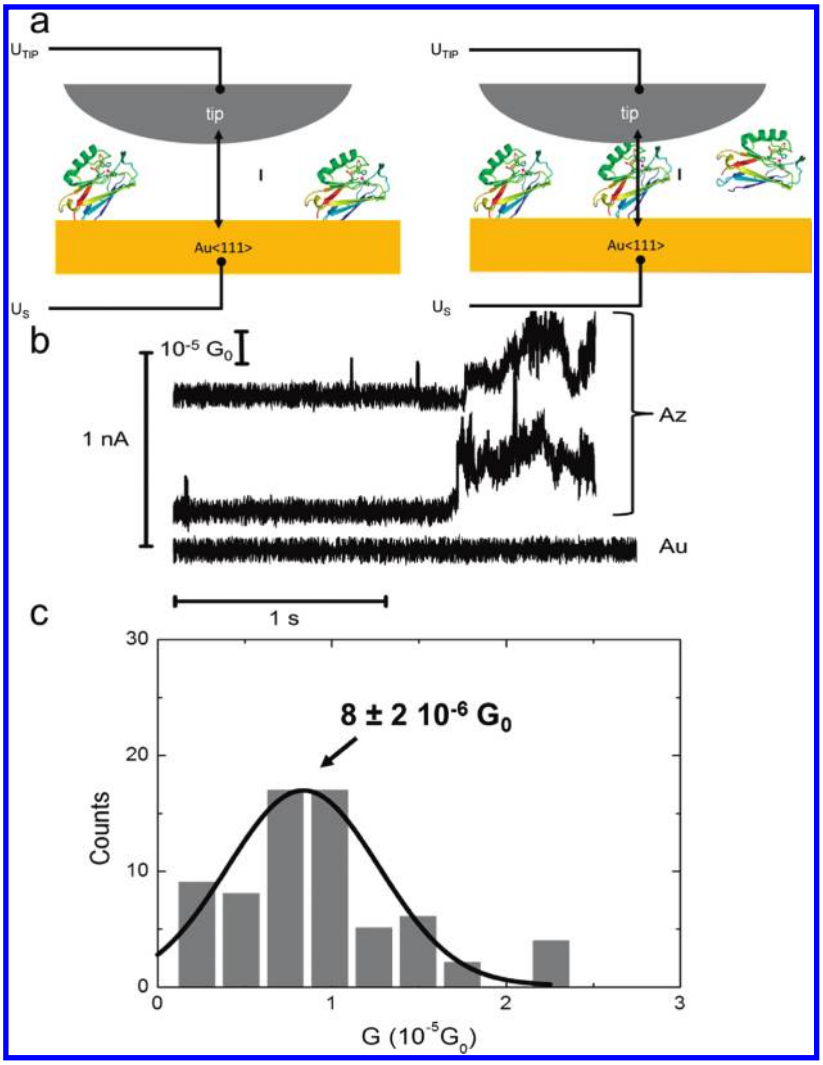

Figure 3. (a) Diagram illustrating a "blinking" experiment. (b) Example of current vs time traces showing spontaneous single protein junction formation as jumps ("blinks") in the current traces after the feedback loop is turned off. The lower trace corresponds to a control performed on a clean gold surface. Traces have been vertically offset for clarity. (c) Conductance histogram built from 75 "blinks" traces. The black line is a Gaussian fit centered at $(8.5 \pm 2.4) \times 10^{-6} G_0$. The experiments were performed in 50 mM ammonium acetate solution (pH 4.5) at $U_P = -0.1$ V vs SSC, $U_S = 0.2$ V vs SSC, and $U_{bias} = U_P - U_S = -0.3$ V.

azurin[14] and other redox molecules in ECSTM configuration.[46] Conductance modulation of a single-azurin junction is possible thanks to the azurin redox behavior and constitutes a proof-of-concept of a wired single-protein transistor.

In order to directly assess the performance of a single-azurin transistor, it is necessary to form and hold a single-protein junction within a time frame ranging between a few hundred milliseconds to a second, time needed to scan the electrochemical gate and/or bias voltages and characterize in situ its electrical behavior. For this purpose, we used an alternative approach based on current−time recordings at a fixed distance.[19,49] Briefly, after approaching the probe to a tunneling distance with the substrate, the STM feedback was disconnected and the tunneling current was recorded as a function of time (see Figure 3a). Sudden current steps or "blinks" were observed in the current trace, which correspond to individual proteins spontaneously bridging between the probe and substrate electrodes. Figure 3b shows examples of blinking current−time traces obtained using this approach. Traces are vertically offset for clarity. Current blinks are about 0.25 nA in amplitude, in agreement with the current step level observed in previous $I(z)$ traces (see Figure 1). Notice the absence of blinks in control experiments on clean Au (figure 3b, bottom trace). The amplitude of the blink can be also used to calculate single protein conductance using $G = I_{blink}/U_{bias}$ in a moderate bias range (±0.4 V, see Figure S2 in the Supporting Information). Statistical analysis of 75 blinks produces a peak in the conductance histogram (shown in Figure 3c) that can be fitted to a Gaussian distribution function and corresponds to a conductance of $(8 \pm 2) \times 10^{-6} G_0$. This value is in very good agreement with the one obtained by the STM-BJ method and constitutes an independent demonstration of a wired single azurin junction. This agreement suggests that protein conductance is not altered by the STM probe movement during $I(z)$ measurements within a certain z range. The redox gating effect of Figure 2 and its agreement with the blinking experiments at constant z (Figure 4 below) further demonstrate that azurin is electrochemically active and thus functionally intact in both types of measurements.

dx.doi.org/10.1021/nl2028969 |*Nano Lett.* 2012, 12, 2679–2684

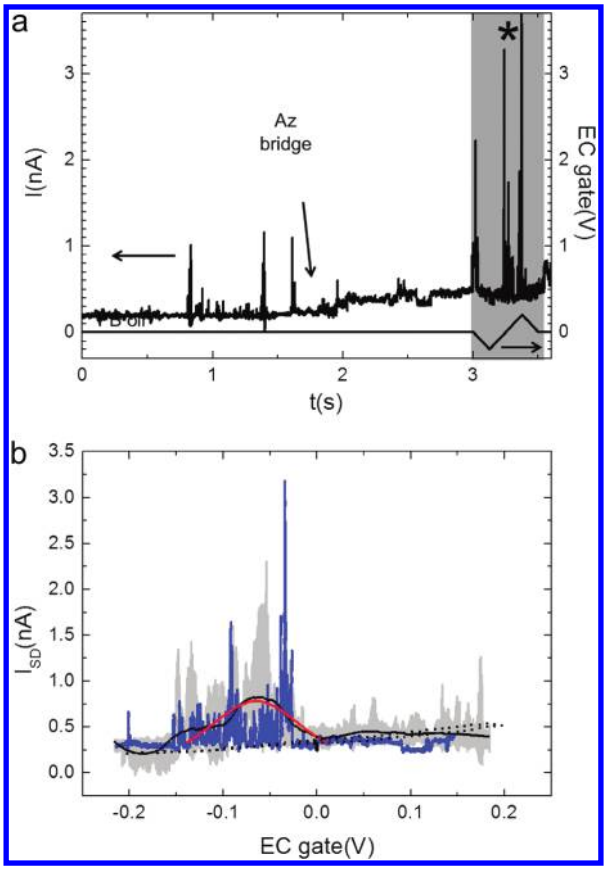

Figure 4. (a) Example of current−time trace (top) where the gate voltage (bottom) is swept (time interval marked in gray) after the spontaneous formation of a single azurin bridge. Current vs time signal refers in the left axis while EC gate voltage vs time signal is in the right axis. (b) An example trace of I_{SD} vs EC gate corresponding to the experiment of (a) is shown in blue. The current vs EC gate voltage average is indicated in black and error bars corresponding to the standard deviation are shown in gray. A fit to the numerical version[45] of the two-step ET model[14] is shown in red. The dotted line shows the average trace obtained in nonredox Zn−azurin control experiments (see also Figure S3 in the Supporting Information). The experiments were performed in 50 mM ammonium acetate solution (pH 4.55) at initial U_P = −0.3 V vs SSC, U_S = 0 V vs SSC, and constant $U_{bias} = U_P - U_S$ = −0.3 V.

Protein bridge formation in $I(t)$ recordings can be automatically detected with a current threshold, which allows triggering direct electrical measurement and manipulation experiments in individual protein junctions. Single-molecule conductance fluctuations are inherent in these current traces (Figure 3b) and the amplitude of these fluctuations is within the experimental dispersion observed as the peak width in the previous histograms (Figure 1). Junctions can also be broken deliberately by ramping the z position as in a "pulling" experiment, which give further evidence that these conductance measurements correspond to individual single-protein junctions (Figure S4, Supporting Information). As pointed out above, current−voltage characteristics of individual single-protein junctions can be recorded by this method by ramping the bias voltage (Figure S2, Supporting Information). More interestingly, the junction current can be modulated or "electrochemically gated" by ramping probe and sample potentials at constant bias voltage (Figure 4). This setup is analogous to a FET where the source and drain electrodes are constituted by the ECSTM probe and substrate electrodes, and the gate electrode corresponds in practice to the reference electrode (whose potential is added to both U_S and U_P in most ECSTM bipotentiostats). An example of source−drain current (I_{SD}) trace is shown in the blue line of Figure 4b as a function of the EC gate displaying a maximum at the potential corresponding to the alignment between the Fermi levels of the electrodes and redox energy level of the protein (−0.08 V). This result is homologous to the one obtained from averaged conductance histograms in Figure 2b and confirms that azurin is electrochemically active in junctions formed with both $I(z)$ and blinking measurements. Current fluctuations in the blue trace of Figure 4b are characteristic of single protein recordings and can be partially averaged out by repeating electrochemical gating experiments in several blinking events (black trace in Figure 4b is the 10 curves average). The current maximum is evident in the averaged trace and indicates negative differential resistance of the single protein junction. Fitting the maximum to a two-step ET model[14] (red trace in Figure 4b) yields similar parameters as in the STM-BJ approach (λ = 0.3 eV, ξ = 1, γ = 0.55). Note that no gate effect is obtained in control experiments with nonredox Zn−azurin (dashed line in Figure 4b and Figure S5 in the Supporting Information). Redox gating of individual proteins display an average on/off ratio of about 3 and a substantial variability across molecules that could be reduced in part by improving the anchoring chemistry of the molecular wiring between azurin and the ECSTM probe.

In summary, the conductance and transistor-like behavior of single protein junctions were studied for the first time using STM-BJs. The conductance and on/off gating ratios obtained compare well with previous studies using "tunneling" junctions where proteins were attached either to the substrate[14] or to the STM probe.[36] The STM-BJ approach has the advantage of an enhanced protein confinement between the electrodes and a high rate of successful recordings per experiment that allows statistical analysis. Current−time experiments at constant distance[19] reveal blinking events that correspond to the transient binding of individual proteins bridging the two electrodes. Current−voltage characteristics of azurin under this configuration reveal negative differential resistance and demonstrate that biomolecular transistors can be built using single metalloprotein junctions. Thus, the tools of molecular electronics[50] have been successfully extended to characterize at the single molecule level the ET properties of redox proteins interesting for biosensing[2] and bioelectronics[6] and to assess the electronic performance of novel devices based on single proteins.

■ ASSOCIATED CONTENT

Supporting Information. Experimental methods, multiple alignments with metal binding peptides, single protein current voltage experiments, linear conductance histograms as a function of substrate potential, single protein "pulling" experiments, and non-redox Zn−azurin EC gate control experiments. This material is available free of charge via the Internet at http://pubs.acs.org.

■ AUTHOR INFORMATION

Corresponding Author
*E-mail: pau@icrea.cat.

■ ACKNOWLEDGMENT

This work was supported in part by Grants PET0808 from the MICINN and 2009-SGR277 from the Generalitat de Catalunya.

J.M.A. acknowledges a fellowship of the Generalitat de Catalunya under the BE-DGR 2009 program and I.D.-P. acknowledges a contract from the MICINN under the Ramon y Cajal program. We thank J. Palou for technical assistance, A. Giraudet for help in experimental work, and F. Sanz for helpful discussions.

REFERENCES

(1) Marcus, R. A.; Sutin, N. *Biochim. Biophys. Acta* **1985**, *811* (3), 265–322.
(2) Heller, A.; Feldman, B. *Acc. Chem. Res.* **2010**, *43* (7), 963–973.
(3) Villalonga, R.; Diez, P.; Yanez-Sedeno, P.; Pingarron, J. M. *Electrochim. Acta* **2011**, *56* (12), 4672–4677.
(4) Toghill, K. E.; Compton, R. G. *Int. J. Electrochem. Sci.* **2010**, *5* (9), 1246–1301.
(5) D'Amico, S.; Maruccio, G.; Visconti, P.; D'Amone, E.; Bramanti, A.; Cingolani, R.; Rinaldi, R. *IEE Proc.: Nanobiotechnol.* **2004**, *151* (5), 173–175.
(6) Lee, T.; Kim, S.-U.; Min, J.; Choi, J.-W. *Adv. Mater.* **2010**, *22*, (4), 510-+.
(7) Guo, S.; Dong, S. *TrAC Trends Anal. Chem.* **2009**, *28* (1), 96–109.
(8) Marshall, N. M.; Garner, D. K.; Wilson, T. D.; Gao, Y.-G.; Robinson, H.; Nilges, M. J.; Lu, Y. *Nature* **2009**, *462* (7269), 113–116.
(9) Lancaster, K. M.; George, S. D.; Yokoyama, K.; Richards, J. H.; Gray, H. B. *Nat. Chem.* **2009**, *1* (9), 711–715.
(10) Yang, H.; Luo, G.; Karnchanaphanurach, P.; Louie, T.-M.; Rech, I.; Cova, S.; Xun, L.; Xie, X. S. *Science* **2003**, *302* (5643), 262–266.
(11) Flomenbom, O.; Velonia, K.; Loos, D.; Masuo, S.; Cotlet, M.; Engelborghs, Y.; Hofkens, J.; Rowan, A. E.; Nolte, R. J. M.; Van der Auweraer, M.; de Schryver, F. C.; Klafter, J. *Proc. Natl. Acad. Sci. U.S.A.* **2005**, *102* (7), 2368–2372.
(12) Shi, J.; Dertouzos, J.; Gafni, A.; Steel, D.; Palfey, B. A. *Proc. Natl. Acad. Sci. U.S.A.* **2006**, *103* (15), 5775–5780.
(13) Kuznetsova, S.; Zauner, G.; Aartsma, T. J.; Engelkamp, H.; Hatzakis, N.; Rowan, A. E.; Nolte, R. J. M.; Christianen, P. C. M.; Canters, G. W. *Proc. Natl. Acad. Sci. U.S.A.* **2008**, *105* (9), 3250–3255.
(14) Chi, Q. J.; Farver, O.; Ulstrup, J. *Proc. Natl. Acad. Sci. U.S.A.* **2005**, *102* (45), 16203–16208.
(15) Alessandrini, A.; Corni, S.; Facci, P. *Phys. Chem. Chem. Phys.* **2006**, *8* (38), 4383–4397.
(16) Della Pia, E. A.; Chi, Q. J.; Jones, D. D.; Macdonald, J. E.; Ulstrup, J.; Elliott, M. *Nano Lett.* **2011**, *11* (1), 176–182.
(17) Reed, M. A.; Zhou, C.; Muller, C. J.; Burgin, T. P.; Tour, J. M. *Science* **1997**, *278* (5336), 252–254.
(18) Xu, B. Q.; Tao, N. J. J. *Science* **2003**, *301*, 1221–1223.
(19) Haiss, W.; Nichols, R. J.; van Zalinge, H.; Higgins, S. J.; Bethell, D.; Schiffrin, D. J. *Phys. Chem. Chem. Phys.* **2004**, *6* (17), 4330–4337.
(20) Aviram, A.; Ratner, M. A. *Chem. Phys. Lett.* **1974**, *29* (2), 277–283.
(21) Xu, B. Q. Q.; Li, X. L. L.; Xiao, X. Y. Y.; Sakaguchi, H.; Tao, N. J. J. *Nano Lett.* **2005**, *5* (7), 1491–1495.
(22) Albrecht, T.; Guckian, A.; Ulstrup, J.; Vos, J. G. *Nano Lett* **2005**, *5* (7), 1451–1455.
(23) Xu, B. Q.; Zhang, P. M.; Li, X. L.; Tao, N. J. *Nano Lett.* **2004**, *4* (6), 1105–1108.
(24) Hihath, J.; Xu, B. Q.; Zhang, P. M.; Tao, N. J. *Proc. Natl. Acad. Sci. U.S.A.* **2005**, *102* (47), 16979–16983.
(25) He, J.; Lin, L.; Zhang, P.; Lindsay, S. *Nano Lett.* **2007**, *7* (12), 3854–3858.
(26) Chang, S.; Huang, S.; He, J.; Liang, F.; Zhang, P.; Li, S.; Chen, X.; Sankey, O.; Lindsay, S. *Nano Lett.* **2010**, *10* (3), 1070–1075.
(27) Ron, I.; Pecht, I.; Sheves, M.; Cahen, D. *Acc. Chem. Res.* **2010**, *43* (7), 945–953.
(28) Ron, I.; Sepunaru, L.; Itzhakov, S.; Belenkova, T.; Friedman, N.; Pecht, I.; Sheves, M.; Cahen, D. *J. Am. Chem. Soc.* **2010**, *132* (12), 4131–4140.
(29) Cardamone, D. M.; Kirczenow, G. *Nano Lett.* **2010**, *10* (4), 1158–1162.
(30) Xiao, X. Y.; Xu, B. Q.; Tao, N. J. *J. Am. Chem. Soc.* **2004**, *126* (17), 5370–5371.
(31) Gray, H. B.; Winkler, J. R. *Biochim. Biophys. Acta, Bioenerg.* **2010**, *1797* (9), 1563–1572.
(32) Adman, E. T.; Jensen, L. H. *Isr. J. Chem.* **1981**, *21* (1), 8–12.
(33) Artés, J. M.; Díez-Pérez, I.; Sanz, F.; Gorostiza, P. *ACS Nano* **2011**, *5* (3), 2060–2066.
(34) Friis, E. P.; Andersen, J. E. T.; Madsen, L. L.; Moller, P.; Ulstrup, J. *J. Electroanal. Chem.* **1997**, *431* (1), 35–38.
(35) Gray, H. B.; Winkler, J. R. *Chem. Phys. Lett.* **2009**, *483* (1−3), 1–9.
(36) Alessandrini, A.; Salerno, M.; Frabboni, S.; Facci, P. *Appl. Phys. Lett.* **2005**, *86* (13), 133902.
(37) Huang, Z.; Chen, F.; Bennett, P. A.; Tao, N. *J. Am. Chem. Soc.* **2007**, *129* (43), 13225–13231.
(38) Axford, D.; Davis, J. J.; Wang, N.; Wang, D. X.; Zhang, T. T.; Zhao, J. W.; Peters, B. *J. Phys. Chem. B* **2007**, *111* (30), 9062–9068.
(39) Davis, J. J.; Wang, N.; Morgan, A.; Tiantian, Z.; Jianwei, Z. *Faraday Discuss.* **2005**, No. 131, 167–179.
(40) Seker, U. O. S.; Demir, H. V. *Molecules* **2011**, *16* (2), 1426–1451.
(41) Hines, T.; Diez-Perez, I.; Hihath, J.; Liu, H.; Wang, Z.-S.; Zhao, J.; Zhou, G.; Muellen, K.; Tao, N. *J. Am. Chem. Soc.* **2010**, *132* (33), 11658–11664.
(42) James, G. K.; et al. *Nanotechnology* **2004**, *15* (7), S489.
(43) Reichert, J.; Ochs, R.; Beckmann, D.; Weber, H. B.; Mayor, M.; von Lohneysen, H. *Phys. Rev. Lett.* **2002**, *88* (17), 176804.
(44) Nijhuis, C. A.; Reus, W. F.; Whitesides, G. M. *J. Am. Chem. Soc.* **2010**, *132* (51), 18386–18401.
(45) Li, X.; Hihath, J.; Chen, F.; Masuda, T.; Zang, L.; Tao, N. *J. Am. Chem. Soc.* **2007**, *129* (37), 11535–11542.
(46) Pobelov, I. V.; Li, Z. H.; Wandlowski, T. *J. Am. Chem. Soc.* **2008**, *130* (47), 16045–16054.
(47) Diez-Perez, I.; Li, Z.; Hihath, J.; Li, J.; Zhang, C.; Yang, X.; Zang, L.; Dai, Y.; Feng, X.; Muellen, K.; Tao, N. *Nat. Commun.* **2010**, *1*, DOI: 10.1038/ncomms1029.
(48) Sepunaru, L.; Pecht, I.; Sheves, M.; Cahen, D. *J. Am. Chem. Soc.* **2011**, *133* (8), 2421–2423.
(49) Diez-Perez, I.; Hihath, J.; Lee, Y.; Yu, L. P.; Adamska, L.; Kozhushner, M. A.; Oleynik, I. I.; Tao, N. J. *Nat. Chem.* **2009**, *1* (8), 635–641.
(50) Nichols, R. J.; Haiss, W.; Higgins, S. J.; Leary, E.; Martin, S.; Bethell, D. *Phys. Chem. Chem. Phys.* **2010**, *12* (12), 2801–2815.